Title	Relationship between retinal morphological findings and visual function in age-related macular degeneration.
Author(s)	Akagi-Kurashige, Yumiko; Tsujikawa, Akitaka; Oishi, Akio; Ooto, Sotaro; Yamashiro, Kenji; Tamura, Hiroshi; Nakata, Isao; Ueda-Arakawa, Naoko; Yoshimura, Nagahisa
Citation	Graefe's archive for clinical and experimental ophthalmology (2012), 250(8): 1129-1136
Issue Date	2012-08
URL	http://hdl.handle.net/2433/160377
Right	The final publication is available at www.springerlink.com
Type	Journal Article
Textversion	author

Relationship between Retinal Morphological Findings and Visual Function in Age-Related Macular Degeneration

YUMIKO AKAGI-KURASHIGE, MD; AKITAKA TSUJIKAWA, MD; AKIO OISHI, MD; SOTARO OOTO, MD; KENJI YAMASHIRO, MD; HIROSHI TAMURA, MD; ISAO NAKATA, MD; NAOKO UEDA-ARAKAWA, MD; AND NAGAHISA YOSHIMURA, MD

Department of Ophthalmology and Visual Sciences, Kyoto University Graduate School of Medicine, Kyoto, Japan

Corresponding author: Akitaka Tsujikawa, MD, Department of Ophthalmology, Kyoto University Graduate School of Medicine, Sakyo-ku, Kyoto 606-8507, Japan

Tel: +81-75-751-3260; Fax: +81-75-752-0933; E-mail: tujikawa@kuhp.kyoto-u.ac.jp

Abstract

Background: We aimed to study the retinal morphological findings associated with exudative age-related macular degeneration (AMD) and their association with visual prognosis.

Methods: We retrospectively reviewed the medical records of 96 consecutive patients (96 eyes) with exudative AMD. Retinal structural changes were examined using optical coherence tomography (OCT).

Results: Initial OCT examination showed cystoid macular edema in 18 eyes (18.8%), fibrin exudate in 56 eyes (58.3%), and hyperreflective foci within the neurosensory retina in 78 eyes (81.3%). Upon initial examination, an external limiting membrane (ELM) line was detected under the fovea in 64 eyes (66.7%). Using Pearson's correlation analyses, final visual acuity (VA) was correlated with initial VA (r = 0.61, $p < 0.001$), age (r = 0.34, $p < 0.001$), initial total foveal thickness (r = 0.41, $p < 0.001$), presence of hyperreflective foci (r = 0.40, $p < 0.001$), and detection of a foveal ELM line (r = 0.55, $p < 0.001$). After multiple regression analysis, final VA correlated with initial VA (r = 0.48, $p < 0.001$), initial presence of hyperreflective foci (r = 0.23, $p = 0.054$), and detection of a foveal ELM line (r = 0.36, $p = 0.008$).

Conclusions: In eyes with exudative AMD, final VA was most correlated with initial VA.

In addition, the initial integrity of the foveal outer retina was partially correlated with the visual prognosis. The initial ELM condition was associated with good final VA, while the initial presence of hyperreflective foci in the foveal neurosensory retina was associated with poor final VA.

Keywords: age-related macular degeneration, external limiting membrane, hyperreflective foci, optical coherence tomography, polypoidal choroidal vasculopathy

Introduction

Age-related macular degeneration (AMD) is a leading cause of blindness worldwide in individuals aged more than 50 years [1]. Although treatment for the disease has progressed dramatically after the development of anti-vascular endothelial growth factor (VEGF) therapy, not all patients achieve good vision [2-4]. A combination of photodynamic therapy (PDT) and anti-VEGF therapy is a promising option [5], but it might not markedly alter the prognosis of AMD [6]. Considering both the physical and financial costs of treatment [7], prediction of the visual prognosis at the patients' initial visits would be very useful to both patients and clinicians.

A more detailed evaluation of retinal structure and function is needed to predict visual prognosis [8]. For this purpose, we have been trying to make the best use of optical coherence tomography (OCT). Current models of commercially available spectral-domain OCT instruments provide fine images (up to 5-μm resolution) of the retinal structure [9,10]. Using spectral-domain OCT, Hayashi et al. showed a correlation between retinal structure and function in eyes with AMD that had undergone PDT [11]. In short, the status of the junction between the inner and outer segments of the photoreceptors (IS/OS) [12,13], which is considered to reflect photoreceptor integrity, is associated with visual acuity (VA) [14]. Other authors have confirmed the association of

IS/OS status with VA [15] and with retinal sensitivity as measured using microperimetry [16]. In addition to IS/OS, the status of the external limiting membrane (ELM) has also been reported to be a good indicator of visual function in eyes with AMD [17]. Evaluation of alterations in these retinal layer patterns at the time of the initial examination provides more detailed information about the retinal status [8,18,19].

In addition to the retinal layer pattern, the presence of hyperreflective foci represents another possible predictive factor of VA [18]. Hyperreflective foci are reported to be present in diabetic macular edema [20], retinal vein occlusion [21], and AMD [18], and have been suggested to be subclinical features of lipoprotein extravasation, which implies blood-retinal barrier impairment. Results consistent with this finding have been reported by other authors; the presence of hyperreflective foci is associated with hard exudate deposition [22]. The breakdown of the blood-retinal barrier as well as the accumulation of hard exudates would both be detrimental to eyes with AMD [18].

Based on this structure-function relationship, we hypothesized that there might be a correlation between the pretreatment structure of eyes with AMD, and the visual prognosis. However, to date, limited information is available about predictive factors of visual prognosis among the features obtained from initial OCT sections in exudative AMD

[23-25]. In the study reported herein, we longitudinally investigated OCT images of eyes with AMD throughout the course of anti-VEGF therapy and examined the relationship between pretreatment features seen on OCT images and the visual prognosis.

Material and methods

For this observational study, we retrospectively reviewed the medical records of 96 consecutive patients (96 eyes) with exudative AMD who were seen by the Macula Service in the Department of Ophthalmology at Kyoto University Hospital between January 2008 and October 2009. Inclusion criteria included: (1) symptomatic subfoveal AMD, (2) the presence of choroidal neovascularization (CNV) beneath the foveal center, (3) the presence of macula-related exudative or hemorrhagic features, and (4) a minimum follow-up of 12 months after the initial visit. The current study included eyes with typical AMD and those with polypoidal choroidal vasculopathy (PCV). The diagnosis of PCV was based on indocyanine green angiography, which reveals a branching vascular network that terminates in polypoidal swelling. When both eyes met the inclusion criteria, only the eye with the more active lesion was included in the current study. Eyes with other macular abnormalities (i.e., pathologic myopia, retinal angiomatous proliferation, idiopathic CNV, presumed ocular histoplasmosis, angioid streaks, or other secondary CNV) and those with senile cataracts that resulted in poor-quality OCT images were excluded from the current study. This study was approved by the Institutional Review Board at the Kyoto University Graduate School of Medicine and adhered to the tenets of the Declaration of Helsinki.

At the initial visit, each patient underwent a comprehensive ophthalmologic examination, including measurement of best-corrected VA (using the Landolt C test), determination of intraocular pressure, indirect ophthalmoscopy, slit-lamp biomicroscopy with a contact lens, spectral-domain OCT (Spectralis HRA+OCT; Heidelberg Engineering, Heidelberg, Germany), and fluorescein and indocyanine green angiography (HRA2; Heidelberg Engineering). At each scheduled follow-up visit, each patient underwent a complete ophthalmologic examination, including VA measurement, slit-lamp biomicroscopy, indirect fundus ophthalmoscopy, and OCT examination. Fluorescein and indocyanine green angiography were performed as deemed necessary.

After the initial visit, each eye was treated based on disease activity and VA. Eyes with exudative AMD were treated either with PDT combined with intravitreal injection of an anti-VEGF agent, or with intravitreal injections of anti-VEGF agents alone. After the initial combined therapy, each eye was considered for retreatment with the combined therapy every 3 months if the eye exhibited residual or recurrent polypoidal lesions upon indocyanine green angiography. In eyes treated with intravitreal injections of anti-VEGF agents alone, additional injections were administered on an as-needed basis.

In the current study, we evaluated the OCT images obtained from all eligible patients both quantitatively and qualitatively. In both the initial and final OCT images, we measured total foveal thickness, defined as the distance between the vitreoretinal interface and the retinal pigment epithelium (Figure 1a). Furthermore, we examined the IS/OS line and the ELM to assess outer foveal photoreceptor layer integrity. The status of the IS/OS line and the ELM line under the fovea was defined as either complete or incomplete. OCT images in eyes with exudative AMD often exhibited subretinal fluid and hemorrhages beneath the neurosensory retina. In addition, most OCT images revealed morphological changes in the neurosensory retina. Cystoid spaces and hyperreflective foci were seen in many cases within the neurosensory retina. Fibrin derived from active CNV or polypoidal lesions was observed as amorphous hyperreflective material, not only in the subretinal space but also within the neurosensory retina. Using horizontal and longitudinal OCT sections, we evaluated whether cystoid macular edema, hyperreflective foci, and fibrin exudates were seen within the 1 mm × 1 mm area around the fovea (Figure 1b).

Statistical analysis was performed using software designed for this purpose (IBM SPSS Statistics Desktop, version 19.0.0; IBM Japan, Tokyo, Japan). All values are presented in terms of means and standard deviation. Best-corrected VA was converted to a logarithm of the minimum angle of resolution (logMAR) equivalent for statistical analysis. Values in typical AMD and PCV were compared using the Student's *t*-test. Bivariate relationships were analyzed using the Pearson's correlation coefficient or the Spearman rank correlation coefficient. Stepwise forward multivariate linear regression analyses were also performed to evaluate the contribution of each initially identifiable factor to final VA. A value of $p < 0.05$ was considered statistically significant.

Results

In the current study, 96 eyes from 96 patients (72 men and 24 women) with exudative AMD who were 57–90 years of age (mean, 73.2 ± 8.5 years) were examined (Table 1). Of these 96 eyes, 61 had PCV and 35 had typical AMD. The mean initial VA (logMAR) and foveal thickness were 0.58 ± 0.49 and 422.5 ± 255.9 µm, respectively; there were no significant differences in these parameters between eyes with typical AMD or PCV (p =

0.889, $p = 0.787$). Active CNV lesions were treated with intravitreal injections of anti-VEGF agents in 38 eyes, and with PDT combined with anti-VEGF agents in 37 eyes. No treatments were performed in 21 eyes. The mean number of injections was 4.7 ± 3.2 and mean number of PDT treatments was 1.7 ±1.0. The mean duration from the final treatment to the final examination was 13.4 ± 9.4 months. The mean follow-up period was 24.6 ± 5.7 months.

At the initial visit, all eyes exhibited exudative changes beneath the neurosensory retina derived from active CNV (subretinal fluid and hemorrhage). In addition, most OCT images revealed morphological changes within the neurosensory retina. Cystoid macular edema was observed in 18.8% of eyes. Cystoid spaces were usually observed within neurosensory retinas that were in direct contact with the underlying type 2 CNV, whereas detached retinas were rarely seen in any of the cystoid spaces. In 58.3% of eyes, OCT revealed that the fibrin exudate was an amorphous hyperreflective material within the subretinal space. Fibrin, which was often seen just over the underlying active type 2 CNV or polypoidal lesions, often appeared to infiltrate the overlying neurosensory retina, especially in the outer aspect, resulting in a lack of IS/OS or ELM lines. In these eyes, the ELM seemed to work in some instances as a blocking agent against the exudates (Figure 2). In 81.3% of eyes, intraretinal hyperreflective foci were seen within the neurosensory retina. Intraretinal hyperreflective foci were frequently seen throughout the entire outer retina, not only outside but also beyond the ELM (Figures 1 and 2). In our patients, the integrity of the inner and outer segments of the foveal photoreceptor cells appeared to be compromised due to exudative change from the CNV. At the initial examination, foveal ELM was seen in 66.7% of the eyes examined, whereas foveal IS/OS was seen in only 22.9% of the eyes examined.

Table 2 shows the correlations of initial VA with other measurements obtained at the initial examination. Both the total foveal thickness and the presence of cystoid macular edema were correlated with initial VA (r = 0.39, $p < 0.001$; r = 0.39, $p < 0.001$). In addition, foveal IS/OS and ELM were also correlated with initial VA (r = 0.35, $p < 0.001$; r = 0.48, $p < 0.001$).

At the final examination, the mean total thickness was significantly reduced to 305.4 ± 224.9 µm ($p < 0.001$), while cystoid macular edema was still seen in 11.5% of the eyes. Despite treatment, restoration of the integrity of the outer photoreceptor layer was limited. Complete detection of the IS/OS and ELM lines was achieved in only 29.1% and 54.2% of eyes, respectively. Table 3 shows the correlations between final VA and other measurements obtained at the final examination. The total foveal thickness and presence of cystoid macular edema were correlated with poor final VA (r = 0.27, p <

0.001; r = 0.33, $p < 0.001$), whereas detection of foveal IS/OS and ELM lines was correlated with good final VA (r = 0.57, $p < 0.001$; r = 0.58, $p < 0.001$). There were no differences in final VA between eyes with typical AMD and PCV ($p = 0.149$).

Table 4 shows the correlations of final VA with measurements obtained at the initial examination (Pearson's correlation analyses); of these, initial VA showed the closest correlation with final VA (r = 0.61, $p < 0.001$). Age (r = 0.34, $p < 0.001$), total foveal thickness (r = 0.40, $p < 0.001$), and the presence of hyperreflective foci or cystoid macular edema (r = 0.26, $p = 0.012$) at the initial visit also correlated with final VA. In addition, the initial detection of the foveal IS/OS and ELM lines was correlated with final VA (r = 0.42, $p < 0.001$; and r = 0.55, $p < 0.001$, respectively). However, there were no differences in final VA between treatment types ($p = 0.637$). Table 5 shows the correlations between VA and the measurements obtained at the initial examination in each group, stratified by treatment. In each group, while the correlations had similar tendencies, some were not statistically significant, perhaps due to the small number of eyes.

Table 6 shows the correlations between final VA and the measurements obtained at the initial examination after multiple regression analysis. By multiple regression analysis, final VA was correlated with initial VA (r = 0.48, $p < 0.001$) and the detection of a foveal ELM line (r = 0.33, $p = 0.008$). The initial presence of cystoid macular edema was associated with initial poor VA (r = 0.39, $p < 0.001$), but had no significant correlation with final visual function. On the other hand, the initial presence of hyperreflective foci had no significant correlation with initial VA (r = 0.11, $p = 0.261$), but showed a marginal correlation with final VA (r = 0.23, $p = 0.054$).

Discussion

In the present study, we evaluated the morphological findings of the retina associated with exudative AMD and found that initial ELM status and the presence of hyperreflective foci are associated with the visual prognosis. Although the predictive power was inferior to that of initial VA, these parameters at the time of the initial examination can be of help in predicting the visual prognosis.

Although both ELM and IS/OS status were correlated with visual prognosis in bivariate relationship analysis, the multiple regression model showed that only ELM, and not IS/OS status, contributes to visual prognosis. This finding can be explained, at least in part, by the previously held notion that the IS/OS change is too sensitive for use in the evaluation of diseases that cause severe retinal damage, such as exudative AMD [17].

In the current study, of the 96 eyes, IS/OS and ELM lines just beneath the fovea were confirmed in 22 eyes (22.9%) and 64 eyes (66.7%), respectively, suggesting that the IS/OS is impaired relatively early in the course of AMD. In fact, the ELM line was always confirmed when an IS/OS line was detectable. This finding is consistent with the findings of previous studies that examined other macular diseases (e.g., macular hole [26], retinal detachment [27]). Taken together, these facts indicate that the IS/OS is more susceptible and is disrupted in earlier stages than is the ELM. Photoreceptor damage appears as disruption of the IS/OS at first and subsequently of the ELM in these conditions, so the evaluation of the ELM and of the IS/OS depends on the severity of the disease.

An intact ELM might indicate the preservation of the anatomic barrier as well as photoreceptor integrity. The ELM consists of the zonula adherens between the Müller cells and the photoreceptors at the base of the outer segments; this junction is not as tight as that of the zonula occludens, but it does limit the movement of large molecules [28]. As shown in Figure 2, some eyes demonstrated termination of subretinal fibrin at the ELM border, suggesting that the ELM actually acts as a barrier to subretinal proteins or lipids. The prevention of molecular invasion and the subsequent retinal fluid accumulation would have beneficial effects on visual prognosis, providing another reason to study ELM status and its relationship with visual prognosis.

The present study also showed that hyperreflective foci could possibly predict vision, as the presence of hyperreflective foci was negatively associated with the visual prognosis. Although hyperreflective foci are not a functional retinal component and subfoveal hard exudate accumulation was not a cause of poor visual prognosis, we believe that the presence of hyperreflective foci are a hallmark of blood-retinal barrier function, and thus reflect visual outcome. Hyperreflective foci were visible before treatment in many eyes (81.3%) but tended to disappear as the exudative changes improved (40.6% at final examination). An earlier report also suggested that the presence of hyperreflective foci reflects blood-retinal barrier impairment [20]. It is possible that eyes with hyperreflective foci at the initial examination had more active CNV and more severe blood-retinal barrier damage. In other words, the small percentage of cases without hyperreflective foci had milder CNV and milder blood-retinal barrier damage; this difference in the degree of blood-retinal barrier damage might have affected visual prognosis.

There are many limitations to the present study, including the retrospective study design, the relatively small study population from a single institution, and the variety of treatment regimens used. While the heterogeneity in disease types might have affected the results, there were no differences in initial and final VA between eyes with typical AMD and PCV. In the current study, eyes with exudative AMD were treated with intravitreal injections of anti-VEGF agents with or without PDT. When stratified by treatment, the correlations showed similar tendencies, some of which were not statistically significant, perhaps due to the small number of eyes. Eyes treated with combination therapy showed the lowest association between the initial condition of the outer retina and final VA. While the phototoxic effect of PDT might be involved in this low correlation, the exact reason is not unclear. It is possible that the treatment regimen used have some effect on the visual prognosis.

Another limitation is the very nature of OCT examinations. The device used depicts only a difference in light reflectance. Furthermore, we are not completely sure what the presence of an intact ELM or hyperreflective foci implies. Both of these are issues that need to be addressed in future studies. Although initial VA is most strongly associated with the visual prognosis, the initial condition of the outer retina may be of help in predicting the visual prognosis in eyes with AMD. This information will help clinicians provide appropriate information to their patients. A further prospective study is necessary to establish the factors that predict visual prognosis in eyes with exudative AMD.

References

1. Yannuzzi LA, Friedman R, Fine SL, Gass JDM, Gitter KA, Orth DH, Singerman LJ (1988) Symposium on age-related macular degeneration. Bull N Y Acad Med 64: 955–1013
2. Rosenfeld PJ, Brown DM, Heier JS, Boyer DS, Kaiser PK, Chung CY, Kim RY (2006) Ranibizumab for neovascular age-related macular degeneration. N Engl J Med 355: 1419–1431
3. Brown DM, Kaiser PK, Michels M, Soubrane G, Heier JS, Kim RY, Sy JP, Schneider S (2006) Ranibizumab versus verteporfin for neovascular age-related macular degeneration. N Engl J Med 355: 1432–1444
4. Brown DM, Michels M, Kaiser PK, Heier JS, Sy JP, Ianchulev T (2009) Ranibizumab versus verteporfin photodynamic therapy for neovascular age-related macular degeneration: two-year results of the ANCHOR study. Ophthalmology 116: 57–65
5. Heier JS, Boyer DS, Ciulla TA, Ferrone PJ, Jumper JM, Gentile RC, Kotlovker D, Chung CY, Kim RY (2006) Ranibizumab combined with verteporfin photodynamic therapy in neovascular age-related macular degeneration: year 1 results of the FOCUS Study. Arch Ophthalmol 124: 1532–1542

6. Schmidt-Erfurth UM, Pruente C (2007) Management of neovascular age-related macular degeneration. Prog Retin Eye Res 26: 437–451

7. Oishi A, Mandai M, Nishida A, Hata M, Matsuki T, Kurimoto Y (2011) Remission and dropout rate of anti-VEGF therapy for age-related macular degeneration. Eur J Ophthalmol, in press

8. Coscas G, Coscas F, Vismara S, Zourdani A, Li Calzi CI (2009) OCT interpretation. In: Coscas G, Coscas F, Vismara S, Zourdani A, Li Calzi CI (eds) Optical coherence tomography in age-related macular degeneration. Springer-Verlag, Heidelberg, pp 97–170

9. Ko TH, Fujimoto JG, Schuman JS, Paunescu LA, Kowalevicz AM, Hartl I, Drexler W, Wollstein G, Ishikawa H, Duker JS (2005) Comparison of ultrahigh- and standard-resolution optical coherence tomography for imaging macular pathology. Ophthalmology 112: 1922–1935

10. Drexler W, Sattmann H, Hermann B, Ko TH, Stur M, Unterhuber A, Scholda C, Findl O, Wirtitsch M, Fujimoto JG, Fercher AF (2003) Enhanced visualization of macular pathology with the use of ultrahigh-resolution optical coherence tomography. Arch Ophthalmol 121: 695–706

11. Hayashi H, Yamashiro K, Tsujikawa A, Ota M, Otani A, Yoshimura N (2009) Association between foveal photoreceptor integrity and visual outcome in neovascular age-related macular degeneration. Am J Ophthalmol 148: 83–89

12. Gloesmann M, Hermann B, Schubert C, Sattmann H, Ahnelt PK, Drexler W (2003) Histologic correlation of pig retina radial stratification with ultrahigh-resolution optical coherence tomography. Invest Ophthalmol Vis Sci 44: 1696–1703

13. Anger EM, Unterhuber A, Hermann B, Sattmann H, Schubert C, Morgan JE, Cowey A, Ahnelt PK, Drexler W (2004) Ultrahigh resolution optical coherence tomography of the monkey fovea. Identification of retinal sublayers by correlation with semithin histology sections. Exp Eye Res 78: 1117–1125

14. Costa RA, Calucci D, Skaf M, Cardillo JA, Castro JC, Melo LA Jr, Martins MC, Kaiser PK (2004) Optical coherence tomography 3: Automatic delineation of the outer neural retinal boundary and its influence on retinal thickness measurements. Invest Ophthalmol Vis Sci 45: 2399–2406

15. Sayanagi K, Sharma S, Kaiser PK (2009) Photoreceptor status after antivascular endothelial growth factor therapy in exudative age-related macular degeneration. Br J Ophthalmol 93: 622–626

16. Landa G, Su E, Garcia PM, Seiple WH, Rosen RB (2011) Inner segment-outer segment junctional layer integrity and corresponding retinal sensitivity in dry and wet forms of age-related macular degeneration. Retina 31: 364–370

17. Oishi A, Hata M, Shimozono M, Mandai M, Nishida A, Kurimoto Y (2010) The significance of external limiting membrane status for visual acuity in age-related macular degeneration. Am J Ophthalmol 150: 27–32

18. Coscas G, Coscas F, Vismara S, Zourdani A, Li Calzi CI (2009) Clinical features and natural history of AMD. In: Coscas G, Coscas F, Vismara S, Zourdani A, Li Calzi CI (eds): Optical coherance tomography in age-related macular degeneration. Springer-Verlag, Heidelberg, pp 171–274

19. Coscas F, Coscas G, Souied E, Tick S, Soubrane G (2007) Optical coherence tomography identification of occult choroidal neovascularization in age-related macular degeneration. Am J Ophthalmol 144: 592–599

20. Bolz M, Schmidt-Erfurth U, Deak G, Mylonas G, Kriechbaum K, Scholda C (2009) Optical coherence tomographic hyperreflective foci: a morphologic sign of lipid extravasation in diabetic macular edema. Ophthalmology 116: 914–920

21. Ogino K, Murakami T, Tsujikawa A, Miyamoto K, Sakamoto A, Ota M, Yoshimura N (2011) Characteristics of optical coherence tomographic hyperreflective foci in retinal vein occlusion. Retina, in press
22. Ota M, Nishijima K, Sakamoto A, Murakami T, Takayama K, Horii T, Yoshimura N (2010) Optical coherence tomographic evaluation of foveal hard exudates in patients with diabetic maculopathy accompanying macular detachment. Ophthalmology 117: 1996–2002
23. Shah AR, Del Priore LV (2009) Natural history of predominantly classic, minimally classic, and occult subgroups in exudative age-related macular degeneration. Ophthalmology 116: 1901–1907
24. Kaiser PK, Brown DM, Zhang K, Hudson HL, Holz FG, Shapiro H, Schneider S, Acharya NR (2007) Ranibizumab for predominantly classic neovascular age-related macular degeneration: subgroup analysis of first-year ANCHOR results. Am J Ophthalmol 144: 850–857
25. Boyer DS, Antoszyk AN, Awh CC, Bhisitkul RB, Shapiro H, Acharya NR (2007) Subgroup analysis of the MARINA study of ranibizumab in neovascular age-related macular degeneration. Ophthalmology 114: 246–252

26. Theodossiadis PG, Grigoropoulos VG, Theodossiadis GP (2011) The significance of the external limiting membrane in the recovery of photoreceptor layer after successful macular hole closure: a study by spectral domain optical coherence tomography. Ophthalmologica 225: 176–184

27. Wakabayashi T, Oshima Y, Fujimoto H, Murakami Y, Sakaguchi H, Kusaka S, Tano Y (2009) Foveal microstructure and visual acuity after retinal detachment repair: imaging analysis by Fourier-domain optical coherence tomography. Ophthalmology 116: 519–528

28. Marmor MF (1999) Mechanisms of fluid accumulation in retinal edema. Doc Ophthalmol 97: 239–249

Figure Legends

Fig. 1. **A.** Horizontal image of the fovea obtained using optical coherence tomography (OCT) of an eye with active exudative age-related macular degeneration. Using an initial OCT image, 3 measurements were made in the fovea, including total foveal thickness, continuity of the external limiting membrane (ELM; white arrowheads), and continuity of the junction between the inner and outer photoreceptor segments (IS/OS; yellow arrowheads). **B.** Cross-sectional image of the foveal region obtained using OCT. Using these OCT sections, we determined whether cystoid macular edema (white arrow), hyperreflective foci (yellow arrows), or fibrin exudate (yellow arrowheads) were seen within the 1 mm × 1 mm square area around the fovea.

Fig. 2. Changes in retinal structure seen in polypoidal choroidal vasculopathy. **A.** Initial fluorescein angiography. **B.** Initial indocyanine green angiography shows numerous polypoidal lesions. **C.** Initial fundus photograph exhibiting reddish-orange nodules and an adjacent detachment of the pigment epithelium. **D.** Fundus photograph at final visit. **E.** Sectional image obtained using optical coherence tomography (OCT) at the initial visit. Numerous hyperreflective foci (yellow arrows), as well as subretinal fluid/fibrin (yellow asterisk) are seen. The fibrin appears to have infiltrated the outer

retina but appears to be blocked at the external limiting membrane (white arrowheads). The structure of the neurosensory retina seems to be relatively well preserved. The line of the external limiting membrane is detectable under the fovea. The visual acuity was 0.3 by the Landolt chart. **F.** Sectional image obtained using OCT at the final visit. The visual acuity was 0.9 by the Landolt chart.

Fig. 3. Changes in retinal structure seen in typical age-related macular degeneration. **A.** Initial fluorescein angiography shows minimally classic choroidal neovascularization (CNV). **B.** Initial indocyanine green angiography. **C.** Fundus photograph at initial visit shows subfoveal exudate with surrounding subretinal hemorrhage. **D.** Fundus photograph at final visit shows subfoveal fibrous tissue. **E.** Sectional image obtained using optical coherence tomography (OCT) at the initial visit. Hyperreflective foci (yellow arrows) and cystoid macular edema (white arrow) are seen within the neurosensory retina. Subretinal fluid/fibrin (yellow asterisk) is seen subfoveally. The line of the external limiting membrane is not detectable under the fovea. Visual acuity was 0.2 by the Landolt chart. **F.** Sectional image obtained using OCT at the final visit. Sectional OCT image at 20 months shows thick subfoveal deposit. The visual acuity was 0.1 by the Landolt chart.

Table 1. Characteristics of the study population

Number of eyes	96
Age (years; mean [SD[a]])	73.2 (8.5)
Gender (women/men)	24/72
Initial examination	
Visual acuity (logMAR[b]; mean [SD])	0.58 (0.49)
Total foveal thickness (µm; mean [SD])	422.5 (255.9)
Detection of IS/OS[c] under the fovea (complete/incomplete)	22/74
Detection of ELM[d] under the fovea (complete/incomplete)	64/32
Cystoid macular edema, number of eyes (%)	18 (18.8)
Hyperreflective foci, number of eyes (%)	78 (81.3)
Fibrin, number of eyes (%)	56 (58.3)
Follow-up (months; mean [SD])	24.6 (5.7)
Treatment	
Photodynamic therapy (%)	37 (38.5)
Anti-vascular endothelial growth factor therapy (%)	38 (39.6)
Final examination	
Visual acuity (logMAR; mean [SD])	0.65 (0.61)
Total foveal thickness (µm; mean [SD])	305.4 (224.9)
Detection of IS/OS under the fovea (complete/incomplete)	28/68
Detection of ELM under the fovea (complete/incomplete)	52/44
Cystoid macular edema, number of eyes (%)	11 (11.5)
Hyperreflective foci, number of eyes (%)	39 (40.6)
Fibrin, number of eyes (%)	22 (22.9)

[a]SD, standard deviation; [b]logMAR, logarithm of the minimum angle of resolution; [c]IS/OS, junction between the inner and outer photoreceptor segments; [d]ELM, external limiting membrane

Table 2. Association between initial visual acuity and other measurements obtained at initial examination

	r	*p* value
Age	0.20	0.048
Gender	0.03	0.782
Diabetes mellitus	0.04	0.720
Hypertension	0.08	0.413
Smoking	0.09	0.370
Type of disease	0.03	0.787
Total foveal thickness	0.39	<0.001
Cystoid macular edema	0.39	<0.001
Hyperreflective foci	0.11	0.261
Fibrin	0.05	0.603
Detection of IS/OS[a] under the fovea	0.35	<0.001
Detection of ELM[b] under the fovea	0.48	<0.001

[a]IS/OS, junction between the inner and outer photoreceptor segments; [b]ELM, external limiting membrane

Table 3. Association between final visual acuity and other measurements obtained at final examination

	r	*p* value
Age	0.34	<0.001
Gender	0.03	0.770
Follow-up period	0.03	0.787
Diabetes mellitus	0.06	0.589
Hypertension	0.02	0.827
Smoking	0.01	0.908
Total foveal thickness	0.27	<0.001
Cystoid macular edema	0.33	<0.001
Hyperreflective foci	0.16	0.120
Fibrin	0.12	0.258
Detection of IS/OS[a] under the fovea	0.57	<0.001
Detection of ELM[b] under the fovea	0.58	<0.001

[a]IS/OS, junction between the inner and outer photoreceptor segments; [b]ELM, external limiting membrane

*Fisher's Least Significant Difference test

Table 4. Associations between final visual acuity and measurements obtained at initial examination and during treatment

	r	*p* value
Age	0.34	<0.001
Gender	0.03	0.770
Diabetes mellitus	0.06	0.589
Hypertension	0.02	0.827
Smoking	0.01	0.908
Type of disease	0.15	0.149
Visual acuity (logMAR[a])	0.61	<0.001
Total foveal thickness	0.40	<0.001
Cystoid macular edema	0.34	<0.001
Hyperreflective foci	0.26	0.012
Fibrin	0.06	0.513
Detection of IS/OS[b] under the fovea	0.42	<0.001
Detection of ELM[c] under the fovea	0.55	<0.001
Treatment	-	0.637*

[a]logMAR, logarithm of the minimum angle of resolution; [b]IS/OS, junction between inner and outer segments of the photoreceptors; [c]ELM, external limiting membrane

*Fisher's Least Significant Difference test

Table 5. Association between final visual acuity and other measurements obtained at initial examination in each group, stratified by treatment

	No treatment (n = 21)		Photodynamic therapy with anti-VEGF agents (n = 37)		Anti-VEGF[a] agents (n = 38)	
	r	*p* value	r	*p* value	r	*p* value
Age	0.50	0.022	0.32	0.058	0.27	0.106
Gender	0.40	0.073	0.23	0.177	0.03	0.869
Diabetes mellitus	0.09	0.712	0.27	0.101	0.22	0.175
Hypertension	0.13	0.576	0.15	0.367	0.04	0.793
Smoking	0.02	0.926	0.12	0.481	0.14	0.397
Visual acuity (logMAR[b])	0.76	<0.001	0.48	0.003	0.62	<0.001
Total foveal thickness	0.45	0.042	0.36	0.029	0.40	0.013
Cystoid macular edema	NA	NA	0.26	0.117	0.49	0.002
Hyperreflective foci	0.38	0.090	0.01	0.968	0.28	0.093
Fibrin	0.01	0.957	0.07	0.666	0.12	0.469
Detection of IS/OS[c] under the fovea	0.47	0.034	0.32	0.055	0.46	0.004
Detection of ELM[d] under the fovea	0.71	<0.001	0.26	0.117	0.65	<0.001

[a]VEGF, vascular endothelial growth factor; [b]logMAR, logarithm of the minimum angle of resolution; [c]IS/OS, junction between inner and outer photoreceptor segments; [d]ELM, external limiting membrane

No eyes exhibited cystoid macular edema at the initial visit in the no treatment group.

Table 6. Association between final visual acuity and measurements obtained at initial examination, evaluated by multiple regression analysis

	Partial regression coefficient	*p* value
Age	0.01	0.036
Gender	NA[a]	-
Diabetes mellitus	NA	-
Hypertension	NA	-
Smoking	NA	-
Type of disease	NA	-
Visual acuity (logMAR[b])	0.48	<0.001
Total foveal thickness	<0.01	0.292
Cystoid macular edema	0.02	0.856
Hyperreflective foci	0.23	0.054
Fibrin	NA	-
Detection of IS/OS[c] under the fovea	0.13	0.279
Detection of ELM[d] under the fovea	0.33	0.008

[a]NA, not applicable; [b]logMAR, logarithm of the minimum angle of resolution; [c]IS/OS, junction between inner and outer photoreceptor segments; [d]ELM, external limiting membrane

Figure 1
Click here to download high resolution image

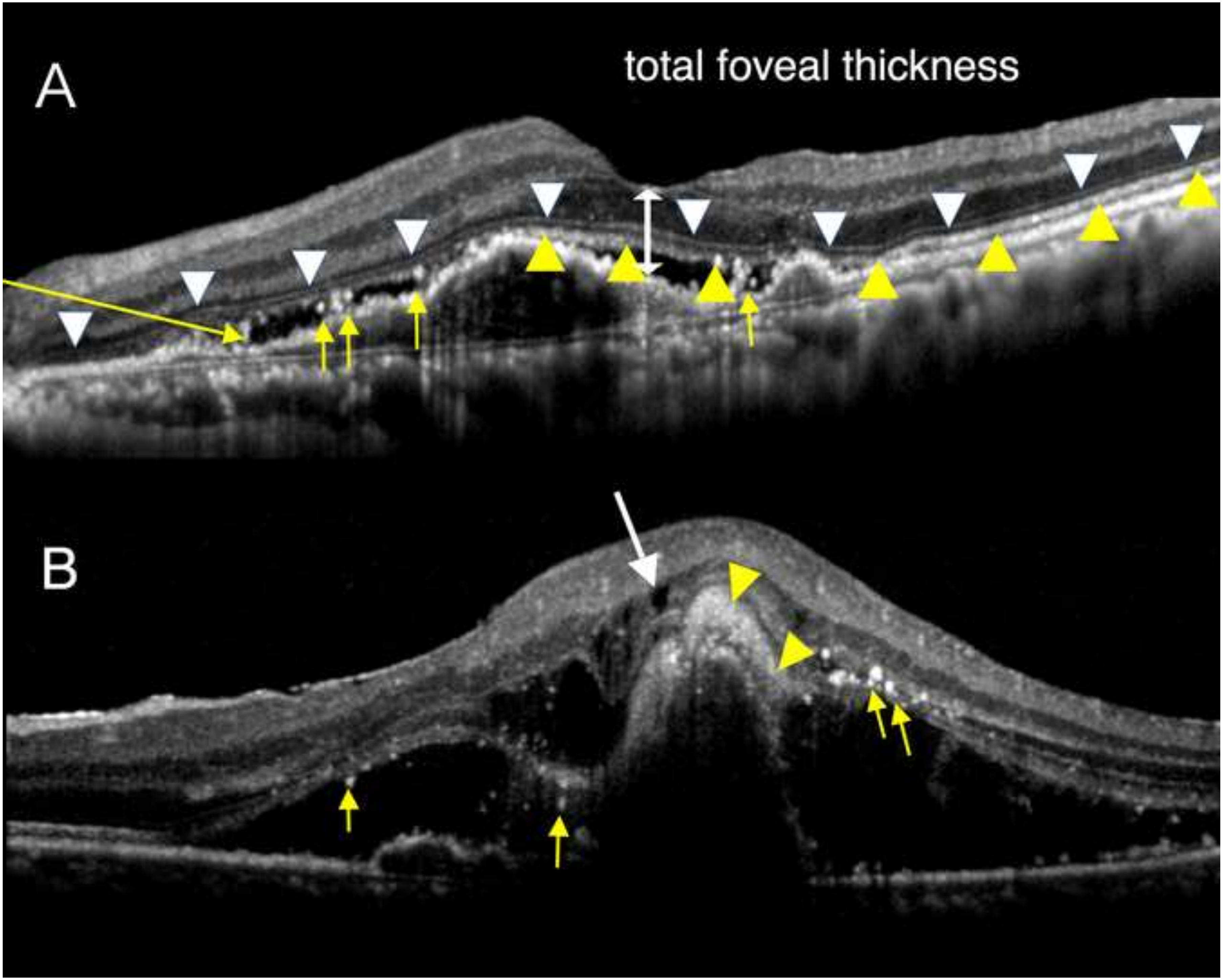

Figure 2

Click here to download high resolution image

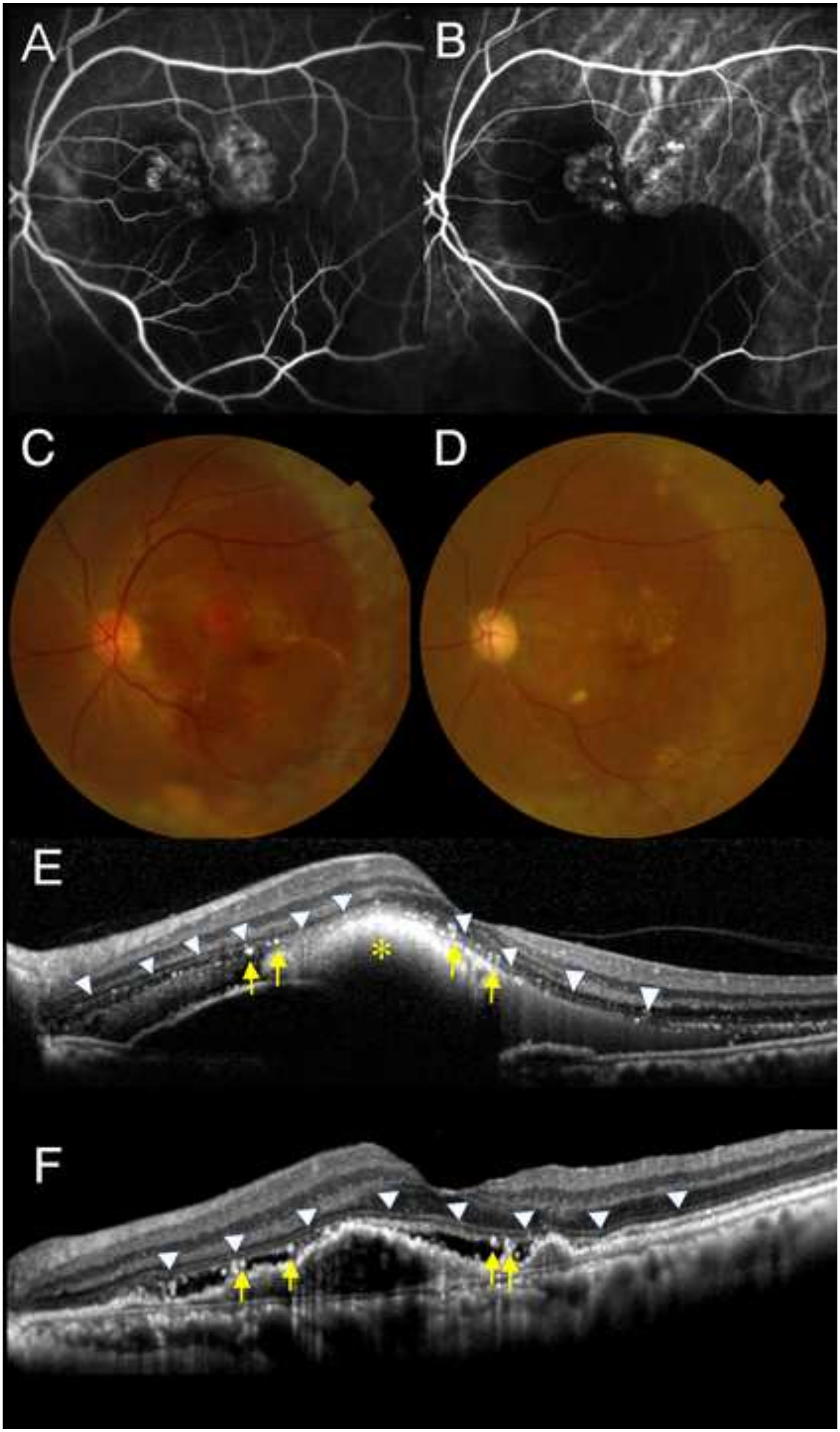

Figure 3
Click here to download high resolution image